Saturation magnetization of ferromagnetic and ferrimagnetic nanocrystals at room temperature

H M Lu, W T Zheng and Q Jiang[1]

Key Laboratory of Automobile Materials (Jilin University), Ministry of Education, and
Department of Materials Science and Engineering, Jilin University, Changchun 130022,
People's Republic of China

E-mail: jiangq@jlu.edu.cn

Abstract
The size-dependent saturation magnetization $M_s(D)$ of ferromagnetic and
ferrimagnetic nanocrystals at room temperature, without free parameters,
has been predicted in terms of a size-dependent cohesive energy model,
where D denotes the diameter of nanoparticles or the thickness of thin films.
The given $M_s(D)$ functions, which are also a function of interface
conditions for substrate supported nanocrystals, drop as D decreases, which
correspond to the available experimental and theoretical results for
ferromagnetic Ni films, Fe, Co, Ni nanoparticles, and ferrimagnetic
γ-Fe_2O_3, Fe_3O_4, $MnFe_2O_4$ and $CoFe_2O_4$ nanoparticles.

1. Introduction

During the past decades, the design, preparation and
characterization of magnetic materials of nanometre sized
scale have been of great interest [1–3]. Magnetic nanoparticles
with unique physical properties have high potential for
applications in diverse areas of high-density perpendicular
recording, colour imaging, ferrofluids, ultrahigh frequency
(300 MHz–3 GHz) devices, magnetic refrigeration and drug
carriers for site-specific drug delivery [4–6]. For instance,
manganese spinel ferrite $MnFe_2O_4$ nanoparticles could be
used for contrast enhancement agents in magnetic resonance
imaging technology [7–10]. Cobalt ferrite $CoFe_2O_4$ is a
promising material in the production of isotropic permanent
magnets, magnetic recording and fluids because it has a very
high cubic magnetocrystalline anisotropy accompanied with a
reasonable saturation magnetization value M_s [11]. $CoFe_2O_4$
has a relatively large magnetic hysteresis in comparison with
the rest of the spinel ferrites [12]. Ferrimagnetic particles,
such as maghemite γ-Fe_2O_3, may be applied in magnetic
recording media and ferrofluids. Magnetic nanoparticles
usually have a single domain magnetic structure and exhibit
unique phenomena such as superparamagnetism and quantum
tunnelling of magnetization. Studying these properties of

nanocrystals provides opportunities to understand magnetic
properties at an atomic level without interference from
complicated domain wall movements, especially to discuss
size-dependent magnetic properties.

M_s, defined as the maximum of the magnetization value
achieved in a sufficiently large magnetic field, is one of
the most important and controversial properties of magnetic
nanocrystals. M_s is a function of measuring temperature T.
It is found that the magnetic moments of Co and Ni clusters
are higher than the corresponding bulk values at zero Kelvin
while they decrease between 82 and 267 K [13, 14]. The
size-enhanced M_s at low temperature can be attributed to the
localized charges that are trapped by the deepened potential
well of the lower-coordinated atoms in the relaxed surface
region [15, 16].

M_s at room temperature decreases sharply with decreasing
crystalline size D, which was first pointed out by Berkowitz
and co-workers in the late sixties [17]. A number of
outstanding theories have been developed to explain the
unusual behaviour of ferromagnetic nanocrystals. A random
canting of the particles surface spins caused by competing
antiferromagnetic exchange interactions at the surface was
first proposed by Coey to explain this reduction [18]. Since
then, the problem has been revisited with arguments in
favour of a surface origin [19] and in favour of a finite size
effect [20]. However, no clear conclusions about it have

---

[1] Author to whom any correspondence should be addressed.

been given yet [2]. Recently, Kodama *et al* proposed a disordered surface spin structure model to illustrate the low saturation magnetization of $NiFe_2O_4$ nanoparticles [21], while Mamiya *et al* attributed the low saturation magnetization of iron nitride ε-Fe_3N nanoparticles to dipolar inter-particle interactions [22]. In addition, when a core-shell structure is assumed where the shell layer (non-magnetic layer) has a constant thickness t and has lower M_s than the corresponding bulk one M_{s0} [7], Tang *et al* derived an empirical relation for size-dependent saturation magnetization $M_s(D)$ [7],

$$M_s(D)/M_{s0} = 1 - 6t/D. \quad (1)$$

Although t in equation (1) is a fitting parameter from the experiments, any attempt to theoretically determine it is rare.

Most recently, $M_s(D)$ suppression at room temperature is also interpreted as a result of the Curie temperature T_c suppression in the surface region [16]. By incorporating the bond order–length–strength (BOLS) correlation mechanism into the Ising convention and the Brillouin function, Zhong *et al* developed a model to examine the size, shape, structure and temperature dependences of M_s of ferromagnetic nanosolids in a unified form, which corresponds directly to the decrease of the atoms' cohesive energy due to the coordination number imperfection of atoms near the surface edge [16,23]. In terms of BOLS correlation, at mid-T region ($k_B T/J_{exc} \sim 6$ with k_B and J_{exc} denoting the Boltzmann constant and the exchange strength), $M_s(D, T)$ can be written as [16,23]

$$\frac{\Delta M_s(D, T)}{M_{s0}(T)} = \alpha(J, T) \frac{\Delta E_{exc}(D)}{E_{exc0}}, \quad (2)$$

where parameter $\alpha(J, T)$ depends on T and the mean angular momentum J of the solid of interest, E_{exc} is the exchange energy with the subscript 0 denoting bulk size, and Δ shows the difference. In reality, reducing particle size enhances the value of J due to the contribution from the charge localization, which suggests taking responsibility of M_s enhancement at a very low temperature [23]. However, the size effect on J becomes insignificant compared with that of E_{exc} at room temperature where E_{exc} dominates the magnetic behaviour. Thus, $\alpha(J, T = 300\,\text{K})$ can be taken as a constant, which has been determined as about four for ferromagnetic nanosolids [23]. Using this equation, good agreement between predictions and experimental or Monte Carlo simulations results for a number of specimens was shown [16,23].

All these models developed from various perspectives can attribute significantly to the understanding of $M_s(D)$ suppression at room temperature. However, the existence of the fitting parameter t in equation (1) degrades its theoretical meaning. Moreover, the substrate effects for thin films are also neglected in the abovementioned theories while nanosolids are usually located on a substrate. Thus, consistent insight and a unified $M_s(D)$ function of ferromagnetic and ferrimagnetic nanocrystals considering both size and substrate effects are highly desirable.

Because $\alpha(J, T)$ in equation (2) is a very complicated function of J [23] while J can be assumed to be independent of D at room temperature as stated above, in this contribution, $M_s(D)$ suppression of ferromagnetic and ferrimagnetic nanocrystals at room temperature is considered.

2. Method

In terms of the BOLS correlation and the Ising model, both T_c and M_s are determined by $E_{exc}(T)$, which is the sum of a portion of the cohesive energy E_{coh} and the thermal vibration energy $E_v(T)$ [24, 25], e.g. $E_{exc}(D, T) = AE_{coh}(D) + E_v(T)$ with A being a coefficient. Based on the mean field approximation and Einstein's relation, $E_v(T) = k_B T$ [25]. On the other hand, $E_v(T)$ required for disordering the exchange interaction is a portion of E_{coh} when $T = T_c$ [25]. Thus, $E_v(T = 300\,\text{K})$ should also be proportional to E_{coh}. Under the consideration that the above energetic relationship remains even when $D \to \infty$, then [25]

$$E_{exc}(D)/E_{exc0} = E_{coh}(D)/E_{coh0}. \quad (3)$$

Note that T does not appear in equation (3) because the concerned temperature in this work has been fixed as the room temperature.

$E_{coh}(D)$ function has been established to have the following form [26]:

$$\frac{E_{coh}(D)}{E_{coh0}} = \left[1 - \frac{1}{(D/D_0) - 1}\right] \exp\left[-\frac{2S_b}{3R} \frac{1}{(D/D_0) - 1}\right], \quad (4)$$

where $S_b = H_v/T_b$ is the bulk solid-vapour transition entropy of crystals with H_v and T_b being the bulk solid-vapour transition enthalpy and the solid-vapour transition temperature, respectively, and R denoting the ideal gas constant. D_0 denotes a critical diameter where $E_{coh}(2D_0) = 0$, namely, the structure of the solid and the vapour is indistinguishable. Accordingly, we have

$$D_0 = ch/2, \quad (5)$$

where h is the atomic or molecular diameter. The constant c ($0 < c \leqslant 1$) shows the normalized surface area where $c = 1$ for low-dimensional materials with free surfaces [26]. If the low-dimensional crystals have interfaces where the atomic potential differs significantly from that of surface atoms, c varies somewhat [27]. For thin films on inert substrates, the chemical interactions between the films and the substrates are Van der Vaals forces while the inner interactions of the films are metallic bonds for metallic thin films or covalent bonds for ceramic thin films. Since the potentials of the Van der Vaals forces are much weaker than metallic or covalent bonds and may be neglected, $c = 1$ for this kind of interface condition and the substrate effects can be neglected, while for metallic films on substrates consisting of metallic or covalent bonds, the interactions between the films and the substrates are comparable with the internal interactions of the films. This case is similar to that where one of the two surfaces of the films disappears and thus $c = 1/2$ (the side surfaces of the thin films are neglected due to the small thickness/area ratio of the films). For more complicated interfaces, c may have other values and could be considered case by case.

It is evident in terms of equation (4) that $E_{coh}(D)/E_{coh0}$ decreases with a decrease in D, which reflects the instability of nanocrystals in comparison with the corresponding bulk crystals. This trend is expected since the surface/volume ratio increases with decreasing size while the surface atoms have lower-coordination numbers and thus higher energetic

states, and consequently $E_{coh}(D)$ increases (the absolute value decreases) [26]. Equation (4) has recently been extended to other cases and its validity is confirmed by experimental results with satisfied consistency [28–30].

Substituting equations (3) and (4) into equation (2), it reads,

$$\frac{M_s(D)}{M_{s0}} = 4\left\{1 - \frac{1}{2D/(ch) - 1}\right\}$$
$$\times \exp\left\{-\frac{2S_b}{3R}\frac{1}{2D/(ch) - 1}\right\} - 3. \tag{6}$$

3. Results

Figure 1 shows a comparison of $M_s(D)/M_{s0}$ functions between the model predictions in terms of equation (6) and the corresponding experimental results for ferromagnetic Fe, Co, and Ni metallic nanoparticles measured by Gong *et al* [31], where the related parameters are listed in table 1. For Fe and Ni nanoparticles, the differences between equation (6) and the corresponding experimental results are smaller than 10%, while for Co, the difference is very large when $D < 30$ nm and the reason may be related to the structural transformation from a hexagonal closed-packed (hcp) structure in the bulk to a face-centred cubic (fcc) one in nanometre size [31]. Since $c = 1$ is taken from figure 1, the decrease in size leads to the strongest drop of $M_s(D)$ in terms of equation (6).
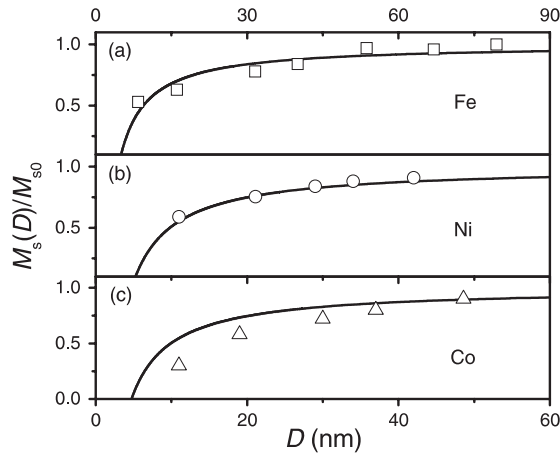

Figure 1. $M_s(D)/M_{s0}$ as a function of D for (*a*) Fe, (*b*) Co and (*c*) Ni ferromagnetic nanoparticles. The solid lines are plotted in terms of equation (6) with $c = 1$ where the symbols □, ○ and △ denote the experimental results [31].

It is known that the disordered structure at the interfaces provides less magnetic moment per unit mass than that of the ferromagnetic core regions, which leads to a decrease in M_s [32]. In contrast with free nanoparticles, where $c = 1$, $c = 1/2$ for the films when the interaction between the surface of the films and the substrate is comparable with the inner interaction of films, $M_s(D)$ suppression of this kind of films will be much weaker than that of free nanoparticles in terms of equation (6) when other parameters are the same.

Figure 2 compares the $M_s(D)/M_{s0}$ function among the model predictions in terms of equation (6) (the solid line), other theoretical results by Zhong *et al* in terms of equation (2) (two-point-segment line) [23] and the corresponding experimental data for Ni films deposited on the glass substrates and on the Si (1 0 0) substrates [33, 34]. It is obvious that the predictions of equation (6) correspond to that of equation (2) with the difference being smaller than 5%. Note that the experimental results (open triangle) show an oscillation behaviour when D is in the range 10–40 nm [33]. Although this was considered to originate from the extraordinary Hall coefficient [33], the Monte Carlo simulations indicated that this abnormal behaviour occurs only in smaller clusters at low temperature [16]. Thus, the deviation from this result and equation (6) at $10 < D < 40$ nm does not reduce the correctness of equation (6). On the other hand, the experimental $M_s(D)$ values of films with $D \leqslant 10$ nm deduced from the magnetic field dependence of the Hall voltage [33] and another experimental result [34] correspond to the model predictions within a deviation of 15%.

A comparison between equation (6) and the corresponding experimental results for $M_s(D)/M_{s0}$ of ferrimagnetic oxides γ-Fe$_2$O$_3$ [17], Fe$_3$O$_4$ [35–37], CoFe$_2$O$_4$ [11, 12] and MnFe$_2$O$_4$ [7, 9, 10] nanoparticles is shown in figure 3. As shown in the figure, the model predictions for γ-Fe$_2$O$_3$, CoFe$_2$O$_4$ and MnFe$_2$O$_4$ are in agreement with experimental results within a difference of 12%, while for Fe$_3$O$_4$, this difference with the corresponding experimental result (shown as △) [35] is only 2%. Although this deviation for another experimental result (shown as ○) [36] is 20%, the calculated particle size of 6 nm is smaller than 9 nm observed from the transmission electron microscopic (TEM) measurement [36]. If the latter is employed, the difference reduces to 10%. The two experimental results (shown as □) measured by Amulevicius *et al* [37] give large distinctness of 45% from equation (6) while one result at $D = 9.5$ nm shows perfect agreement with the model prediction. The sharp drop in $M_s(D)$ reflected in the experimental results [37] is surprising

Table 1. Necessary parameters employed in equation (6) noted that the superscripts denote the numbers of references.

	M_{s0} (emu g^{-1})	H_v (kJ g^{-1} atom^{-1})	T_b (K)	S_b (J g^{-1} atom^{-1} K^{-1})	h (nm)
Fe	171 [31]	347 [42]	3134 [42]	110.7	0.2482 [42]
Co	143 [31]	375 [42]	3200 [42]	117.2	0.2506 [42]
Ni	48.5 [31]	378 [42]	3186 [42]	118.6	0.2492 [42]
γ-Fe$_2$O$_3$	76.0 [17]			13R[a]	0.1850 [39]
Fe$_3$O$_4$	92 [35]			13R[a]	0.1890 [43]
MnFe$_2$O$_4$	80 [7]			13R[a]	0.2293 [8]
CoFe$_2$O$_4$	75 [12]			13R[a]	0.2264 [12]

[a] Since the H_v and T_b values of compounds are unavailable, $S_b \approx 13R$ is employed here as a first order approximation, which is equal to that of the average value of the most elements (70–150 J g^{-1} atom^{-1} K^{-1}) [25, 42].

in contrast to those in other oxides, and the reason remains unknown.

Other theoretical predictions for γ-Fe$_2$O$_3$ and MnFe$_2$O$_4$ in terms of equation (1) with $t = 0.57$ or 0.60 for the former [2, 17] and 0.60 or 0.70 for the latter [7, 10] are also shown in figure 3 for comparison (because the fitting parameters t of Fe$_3$O$_4$ and CoFe$_2$O$_4$ are unavailable to us, similar comparisons are not given for these two oxides). Note that in figure 3(a) the plots in terms of equation (1) with $t = 0.57$ and 0.60 nearly overlap each other; Similarly, in figure 3(d), the broken line with $t = 0.60$ overlaps the solid line by equation (6). Generally, the difference between equations (1) and (6) is smaller than 8%. As we know, these oxides have a collinear ferromagnetic spin structure, which originates from the pinning of the surface spins [21]. The decrease in the sa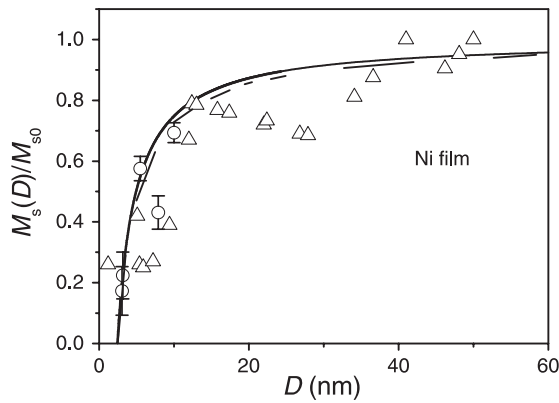turation magnetization can also be explained in terms of its non-collinear spin arrangement at or near the surface of the particle [21]. Such a non-collinear structure attributed to a surface effect will be more pronounced for the smaller particle size.

4. Discussion

Considering a mathematical relation of $\exp(-x) \approx 1-x$ when x is small enough as a first order approximation, equation (6) can be rewritten as,

$$M_s(D)/M_{s0} \approx 1 - ch[2 + 4S_b/(3R)]/D. \qquad (7)$$

The agreements between the model predictions, available experimentally or other theoretical results of $M_s(D)/M_{s0}$ for ferromagnetic and ferrimagnetic nanocrystals as shown in figures 1–3, indicate that the drop of $M_s(D)$ is essentially induced by the increase in the surface–volume ratio, which is the same as the size dependence of any thermodynamic amount [26]. However, as the size of the nanocrystals further decreases to the size being comparable with the atomic or molecular diameter, namely about several nanometres, the difference between equations (6) and (7) becomes evident.

Let equation (7) be equal to zero, or $M_s(D_{crit}) = 0$, where D_{crit} denotes the critical diameter or thickness. Then

$$D_{crit} \approx ch[2 + 4S_b/(3R)]. \qquad (8)$$

Taking the related parameters from table 1 with $c = 1/2$ for the Ni film and 1 for γ-Fe$_2$O$_3$ and MnFe$_2$O$_4$ nanoparticles, $D_{crit} \approx 2.62$, 3.58 and 3.65 nm in terms of equation (8), which correspond to 2.50 nm for the Ni film [23], 3.42 or 3.60 nm for γ-Fe$_2$O$_3$ and 3.60 or 4.20 nm for MnFe$_2$O$_4$ in terms of equation (1) with corresponding t values.
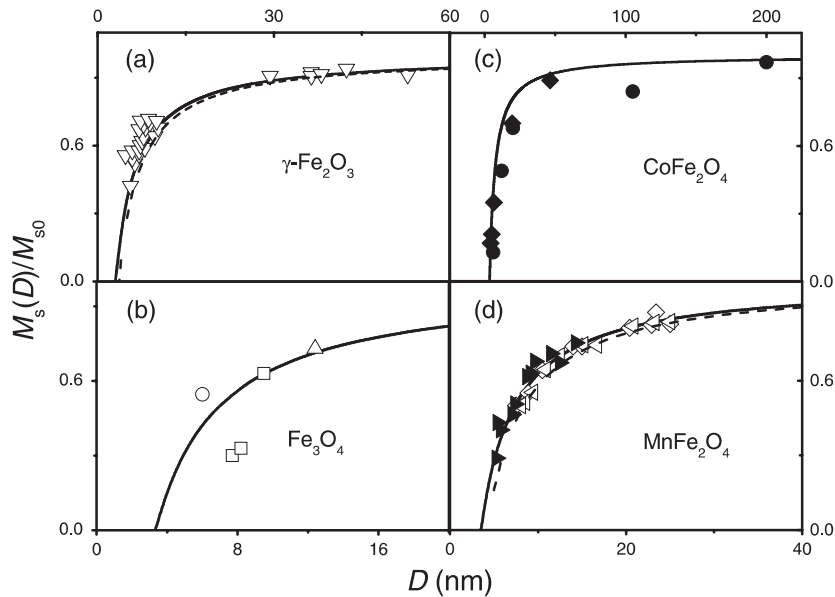

Figure 2. $M_s(D)/M_{s0}$ function of ferromagnetic Ni films. The solid line and two-point-segment line are, respectively, determined by equation (6) with $c = 1/2$ and equation (2) where the symbols $\circ$ and $\triangle$ denote the experimental results for Ni films deposited on glass substrates and Si (1 0 0) substrates [33, 34].

Figure 3. $M_s(D)/M_{s0}$ as a function of D for (a) γ-Fe$_2$O$_3$, (b) Fe$_3$O$_4$ (c) CoFe$_2$O$_4$ and (d) MnFe$_2$O$_4$ ferrimagnetic nanoparticles. The solid lines are determined by equation (6) with $c = 1$ while the two-point-segment lines in (a) and (d) are plotted based on equation (1) with $t = 0.57$ or 0.60 for γ-Fe$_2$O$_3$ [2, 17] and 0.6 or 0.7 for MnFe$_2$O$_4$ [7, 10]. The symbols $\triangleleft$, $\diamond$, $\blacktriangleright$, $\blacklozenge$, $\bullet$, $\triangledown$, $\triangle$, $\circ$ and $\square$ denote the experimental results [7, 9–12, 35–37].
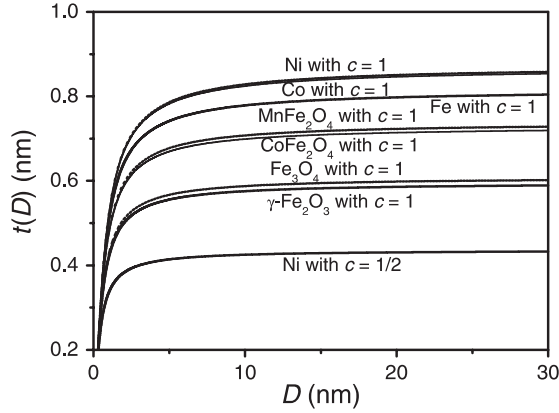
Figure 4. $t(D)$ functions of several ferromagnetic and ferrimagnetic nanocrystals where all the curves are plotted in terms of equation (8).

Moreover, by comparing equation (1) with equation (6), the fitting parameter t can be determined as

$$t(D) = \frac{2D}{3}\left\{1 - \left[1 - \frac{1}{2D/(ch) - 1}\right.\right.$$
$$\left.\left.\times\exp\left[-\frac{2S_b}{3R}\frac{1}{2D/(ch) - 1}\right]\right]\right\}. \quad (9)$$

According to equation (9), t being size dependent is related to four parameters of c, h, S_b and D. When c, h and S_b are certain, t increases with increasing size and approaches a limited value t_{max}, as shown in figure 4 for the materials concerned here. However, this trend is contrary to that for Ni nanoparticles at low temperature (5 K) where the dead layer thickness decreases from 1.83 to 0.76 nm when D increases from 22 to 59 nm [38]. This difference possibly originates from the different temperature range and from the effect of J. As mentioned above, although the size effect of J on M_s at ambient temperature can be neglected [23], when the temperature is very low, e.g. 5 K, this neglect will lead to error. Accordingly, equation (9) is invalid at a very low temperature.

Combining the expression $\exp(-x) \approx 1 - x$ and equation (9), t_{max} is determined as

$$t_{max} \approx ch[1 + 2S_b/(3R)]/3. \quad (10)$$

For a given nanocrystal, the values of S_b and h are certain and t_{max} is thus directly proportional to c. Thus, the $M_s(D)$ suppression of nanoparticles ($c = 1$) is larger than that of thin films having strong interactions with substrates ($c = 1/2$) in terms of equation (7). For instance, $M_s(D)/M_{s0}$ of Ni nanocrystals is about 0.58 with $D \approx 5.5$ nm [31] while it is 0.59 for a Ni film on a Si (1 0 0) substrate with $D \approx 11$ nm [34], as shown in figures 1 and 2, respectively. The strong interaction between films and substrates diminishes the surface effect on M_s. Similar effects on glass transition temperature and Curie transition temperature of thin films have also been observed [25, 27].

As shown in figure 4, the $t(D)$ function is a strong one only when $D < 2$ nm. Since 5 nm $< D <$ 200 nm for the studied nanocrystals as shown in figures 1–3, substituting t_{max} for $t(D)$ is also applicable as a first order approximation. In terms of equation (10) and the data listed in table 1, the t_{max} values of γ-Fe$_2$O$_3$ and MnFe$_2$O$_4$ nanoparticles with $c = 1$ are

determined to be about 0.59 and 0.74 nm, which, respectively, correspond to the fitting results of 0.57 ± 0.2 or 0.60 for the former [2, 17] and 0.60 or 0.70 for the latter [7, 10]. These agreements in reverse confirm the validity of equation (6). Moreover, the thickness of the non-magnetic layer is about the lattice constant of γ-Fe$_2$O$_3$ ($\sim$0.83 nm) or MnFe$_2$O$_4$ ($\sim$0.85 nm) [6, 39], which implies that the magnetic nature of the first crystalline layer of the particles is destroyed by the surface or surface adsorption.

Although $\alpha(J, T = 300\,\text{K}) \approx 4$ in equation (2) was originally determined for ferromagnetic nanosolids, the agreement shown in figure 3 implies that it is also applicable for ferrimagnetic nanocrystals as a first order approximation even if the necessary parameters to determine $\alpha(J, T = 300\,\text{K})$ of ferrimagnetic nanocrystals, e.g. J and E_{coh}, etc, are unavailable. The reason for this sameness is unknown.

Similarly to the relationship between $M_s(D)$ and $E_{exc}(D)$ or $E_{coh}(D)$, $T_c(D)$ has been determined as [16, 23–25]

$$\Delta T_c(D)/T_{c0} = \Delta E_{exc}(D)/E_{exc0} = \Delta E_{coh}(D)/E_{coh0}. \quad (11)$$

In terms of equations (2) and (11) we have

$$\Delta M_s(D)/M_{s0} = 4\Delta T_c(D)/T_{c0} \qquad \text{or}$$
$$M_s(D)/M_{s0} = 4T_c(D)/T_{c0} - 3. \quad (12)$$

Equation (12) indicates that the suppression of $M_s(D)$ at room temperature is about four times that of $T_c(D)$. This can be qualitatively explained as follows: On one hand, the absolute value of $E_{coh}(D)$ drops due to the increase in the portion of the lower-coordination atoms in nanocrystals, which leads to the weakening of inter-spin interaction and thus the suppression of $M_s(D)$ [23]; On the other hand, with rising temperature, increased thermal vibrations tend to counteract the dipole coupling forces in ferromagnetic and ferrimagnetic materials. Consequently, M_s gradually diminishes with increasing T. Since M_s drops to near zero up to T_c [40], M_s seems to be proportional to $(T_c/T - 1)^\beta$ where β denotes an exponent. In fact, a similar expression of $M_s \propto (T_c/T - 1)^{1/2}$ for the ferromagnetic case with $J = 1/2$ has been found by Burns [41]. Because T_c decreases with size while the concerned temperature here has been fixed at room temperature, both T_c/T and M_s reduce. In other words, the effect of decreasing size is equivalent to that of rising temperature. Thus, both effects bring out a stronger suppression of $M_s(D)$ than that of $T_c(D)$ at room temperature where the latter is only induced by reducing size.

5. Conclusions

In summary, the original size-dependent cohesive energy model has been extended to establish a function for M_s suppression of ferromagnetic and ferrimagnetic nanocrystals at room temperature based on relationships among M_s, E_{coh} and E_{exc}. The model, without free parameters, predicts that M_s reduces with size and M_s suppression of free nanoparticles is stronger than that of thin films having strong interactions with substrates. The model predictions are in agreement with the available experimental and other theoretical results for ferromagnetic Fe, Co, Ni nanoparticles, Ni films and ferrimagnetic γ-Fe$_2$O$_3$, Fe$_3$O$_4$, MnFe$_2$O$_4$ and CoFe$_2$O$_4$ nanoparticles.

Together with previous findings of T_c suppression [25], the work here indicates the essentiality of cohesive energy, or equation (4), in describing the effects of size and interface on the magnetic behaviours of ferromagnetic and ferrimagnetic nanocrystals.

Acknowledgments

References

[1] Whitesides G M, Mathias J P and Seto C T 1991 *Science* **254** 1312
[2] Martinez B, Obradors X, Balcells Ll, Rouanet A and Monty C 1998 *Phys. Rev. Lett.* **80** 181
[3] Chen Q and Zhang Z J 1998 *Appl. Phys. Lett.* **73** 3156
[4] Chudnovsky E M and Gunther L 1988 *Phys. Rev. Lett.* **60** 661
[5] Awschalom D D and Divincenzo D P 1995 *Phys. Today* **48** (4) 43
[6] Liu C and Zhang Z J 2001 *Chem. Mater.* **13** 2092
[7] Tang Z X, Sorensen C M, Klabunde K J and Hadjipanayis G C 1991 *Phys. Rev. Lett.* **67** 3602
[8] Kulkarni G U, Kannan K R, Arunarkavalli T and Rao C N R 1994 *Phys. Rev.* B **49** 724
[9] Tang Z X, Sorensen C M, Klabunde K J and Hadjipanayis G C 1991 *J. Appl. Phys.* **69** 5279
[10] Chen J P, Sorensen C M, Klabunde K J, Hadjipanayis G C, Devlin E and Kostikas A 1996 *Phys. Rev.* B **54** 9288
[11] Grigorova M *et al* 1998 *J. Magn. Magn. Mater.* **183** 163
[12] Rajendran M, Pullar R C, Bhattacharya A K, Das D, Chintalapudi S N and Majumdar C K 2001 *J. Magn. Magn. Mater.* **232** 71
[13] Bucher J P, Douglass D C and Bloomfield L A 1991 *Phys. Rev. Lett.* **66** 3052
[14] Apsel S E, Emmert J W, Deng J and Bloomfield L A 1996 *Phys. Rev. Lett.* **76** 1441
[15] Billas I M L, Chatelain A and de Heer W A 1994 *Science* **265** 1682
[16] Zhong W H, Sun C Q, Li S, Bai H L and Jiang E Y 2005 *Acta Mater.* **53** 3207
[17] Berkowitz A E, Shuele W J and Flanders P J 1968 *J. Appl. Phys.* **39** 1261
[18] Coey J M D 1971 *Phys. Rev. Lett.* **27** 1140
[19] Okada T, Sekizawa H, Ambe F and Yamada T 1983 *J. Magn. Magn. Mater.* **31–34** 105
[20] Parker F T, Foster M W, Margulies D T and Berkowitz A E 1993 *Phys. Rev.* B **47** 7885
[21] Kodama R H, Berkowitz A E, McNiff E J and Foner S 1996 *Phys. Rev. Lett.* **77** 394
[22] Mamiya H, Nakatani I and Furubayashi T 1998 *Phys. Rev. Lett.* **80** 177
[23] Zhong W H, Sun C Q and Li S 2004 *Solid State Commun.* **130** 603
[24] Sun C Q, Zhong W H, Li S, Tay B K, Bai H L and Jiang E Y 2004 *J. Phys. Chem.* B **108** 1080
[25] Yang C C and Jiang Q 2005 *Acta Mater.* **53** 3305
[26] Jiang Q, Li J C and Chi B Q 2002 *Chem. Phys. Lett .* **366** 551
[27] Lang X Y and Jiang Q 2004 *Macromol. Rapid Commun.* **25** 825
[28] Xie D, Wang M P and Qi W H 2004 *J. Phys.: Condens. Matter* **16** L401
[29] Lee J G and Mori H 2005 *Eur. Phys. J.* D **34** 227
[30] Liang L H, Yang G W and Li B 2005 *J. Phys. Chem.* B **109** 16081
[31] Gong W, Li H, Zhao Z R and Chen J C 1991 *J. Appl. Phys.* **69** 5119
[32] Tamura K and Endo H 1969 *Phys. Lett.* A **29** 52
[33] Wedler G and Schneck H 1977 *Thin Solid Films* **47** 147
[34] Shi X, Tay B K and Lau S P 2002 *Int. J. Mod. Phys.* B **14** 136
[35] Panda R N, Gajbhiye N S and Balaji G 2001 *J. Alloys Compounds* **326** 50
[36] Liu Z L, Liu Y J, Yao K L, Ding Z H, Tao J and Wang X 2002 *J. Mater. Synth. Process.* **10** 83
[37] Amulevicius A, Baltrunas D, Bendikiene V, Daugvila A, Davidonis D and Mazeika K 2002 *Phys. Status Solidi* a **189** 243
[38] Zhang H T, Wu G, Chen X H and Qiu X G 2006 *Mater. Res. Bull.* **41** 495
[39] Shmakov A N, Kryukova G N, Tsybulya S V, Chuvilin A L and Solovyeva L P 1995 *J. Appl. Crystallogr.* **28** 141
[40] Callister W D 2001 *Fundamentals of Materials Science and Engineering* 5th edn, ed W Anderson (New York: Wiley) p S-291
[41] Burns G 1985 *Solid State Physics* (Orlando, FL: Academic) p 621
[42] Web Elements Periodic Table (http://www.webelements.com/)
[43] Rustad J R, Wasserman E and Felmy A R 1999 *Surf. Sci.* **432** L583